

# Binary subwavelength diffractive-lens design

Joseph N. Mait

*U.S. Army Research Laboratory, AMSRL-SE, 2800 Powder Mill Road, Adelphi, Maryland 20783*

Dennis W. Prather

*Department of Electrical Engineering, University of Delaware, Newark, Delaware 19716*

Mark S. Mirotznik

*Department of Electrical Engineering, The Catholic University of America, Washington, D.C. 20064*

Received May 15, 1998

We present a procedure for the design of binary diffractive lenses with pulse-width-modulated subwavelength features. The procedure is based on the combination of two approximate theories, effective medium theory and scalar diffraction theory, and accounts for limitations on feature size and etch depth imposed by fabrication. A design example is presented. © 1998 Optical Society of America

*OCIS codes:* 050.1970, 050.1940, 050.1960, 220.3630, 220.3620, 260.2110.

Recent research<sup>1-9</sup> has shown that if a binary-phase diffractive optical element has features that are of the order of the illuminating wavelength, the performance limits set by scalar-based diffraction theory can be overcome. In fact, diffraction efficiencies greater than 90% have been predicted for binary gratings that have subwavelength features.<sup>1,4,5</sup>

Primarily because of the availability of tools capable of modeling the behavior of subwavelength diffractive optical elements (SWDOE's), the analysis and design of such elements have concentrated primarily on gratings.<sup>1-7,10</sup> To overcome this limitation we developed numerical routines that use a boundary-element technique to analyze diffraction from finite-extent, aperiodic diffractive optical elements.<sup>11</sup> In this Letter we consider diffractive design, in particular, diffractive lenses.

Our technique is based on the combination of two approximate theories of diffraction, scalar diffraction theory and effective medium theory, and relies on the area modulation of subwavelength features. Area modulation has been used for designing subwavelength gratings<sup>1,4,5</sup> and, more recently, for designing lenses.<sup>8</sup> However, the approach to lens design uses analyses based on gratings and does not directly address the finite and aperiodic nature of lenses. Our approach is to consider directly the spatially varying structure of a diffractive lens and to develop a procedure for the design of arbitrary elements with subwavelength features.

As a first step in the development of our synthesis procedure we consider the diffractive analysis of a general SWDOE illuminated by TE-polarized light wavelength  $\lambda$  and fabricated in a substrate with refractive index  $n_s$  and etch depth  $d$ . Although we use one-dimensional notation to describe the procedure, it is applicable to two-dimensional designs as well.

We assume that the SWDOE surface profile  $t(x)$  is binary:

$$t(x) = df(x), \quad (1)$$

with

$$f(x) = \sum_{\substack{k=1 \\ k \text{ odd}}}^K \text{rect} \left[ \frac{x - (z_{k+1} + z_k)/2}{z_{k+1} - z_k} \right], \quad (2)$$

where the  $z_k$  represent nonoverlapping transition points, i.e., for  $k < l$  and  $z_k < z_l$ , and  $K$  is the total number of transition points, or edges, in the structure. We note that a single binary profile can control only a single polarization independently. However, independent control of both the TE and the TM responses is possible with a multilevel element.<sup>6</sup>

Effective medium theory<sup>12</sup> allows one to predict the permittivity of a periodic structure whose period is less than the wavelength of illumination. To a zeroth-order approximation, the effective permittivity is the average permittivity over a single period. By extending this notion to finite aperiodic structures we can model the relative effective refractive index of  $t(x)$  as

$$n_{\text{TE}}^2(x) = (n_r^2 - 1)g(x) + 1, \quad (3)$$

$$x = [0, W],$$

where  $n_r = n_s/n_0$  is the substrate refractive index relative to the index  $n_0$  of the external environment and  $W$  is the extent of the diffractive element. The index synthesis function  $g(x)$ ,

$$g(x) = f(x) * (1/\Delta)\text{rect}(x/\Delta), \quad (4)$$

is a continuous function bounded by 0 and 1 that we introduce as an aid to design. The convolution, represented by  $*$ , accounts for the effective medium averaging that occurs in each subwavelength region  $\Delta$  of  $t(x)$ ,<sup>8</sup>  $\Delta \leq s_\lambda = \lambda/2n_s$ .

We refer to  $s_\lambda$  as the subwavelength parameter, which was introduced implicitly by Farn.<sup>1</sup> Farn noted

that the diffraction efficiency of gratings tended to increase as their features were decreased to  $s_\lambda$  but remained constant once the features were decreased further. Thus, to ensure high-diffraction design, we use  $s_\lambda$  as an upper limit on subwavelength periods.

Whereas effective medium theory allows one to predict the refractive index of a subwavelength structure, scalar diffraction allows one to predict the phase transformation of a wave field, given a relative index of refraction  $n(x)$ :

$$\theta(x) = \theta_0 \frac{n(x) - 1}{n_r - 1}. \quad (5)$$

Because the relative index  $n(x)$  is bounded by 1 and  $n_r$ ,  $\theta(x)$  is bounded between 0 and  $\theta_0$ , where  $\theta_0$  is related to the element depth  $d$ :

$$\theta_0 = \frac{2\pi d n_0}{\lambda} (n_r - 1). \quad (6)$$

Together Eqs. (3) and (5) allow one to predict the phase transformation  $\theta(x)$ , given a particular profile  $f(x)$ .

To determine a  $g(x)$  that realizes a desired phase transformation  $\theta(x)$  one must invert these equations and combine them:

$$g_{\text{TE}}(x) = \frac{\{(n_r - 1)[\theta(x)/\theta_0] + 1\}^2 - 1}{n_r^2 - 1}. \quad (7)$$

For TM-polarized illumination the relationship between the refractive index and the index synthesis function is

$$\begin{aligned} n_{\text{TM}}^{-2}(x) &= (n_r^{-2} - 1)g(x) + 1, \\ x &= [0, W], \end{aligned} \quad (8)$$

which, in combination with Eq. (5), yields

$$g_{\text{TM}}(x) = \frac{\{(n_r - 1)[\theta(x)/\theta_0] + 1\}^{-2} - 1}{n_r^{-2} - 1}. \quad (9)$$

For Eqs. (7) and (9) to be used properly the desired phase must be quantized to a phase range  $\theta_0$ . We apply a simple quantizer such that input phase values  $\theta(x)$  that lie within the range  $[\theta_c - \theta_0/2, \theta_c + \theta_0/2]$  are offset to  $\theta(x) - \theta_c$ , whereas phase values outside this range are mapped either to 0 or to  $\theta_0$ . We choose the phase value  $\theta_c$  to minimize the mean-square quantization error.

As an example we consider the design of a 20- $\mu\text{m}$  focal-length lens with a 22.72- $\mu\text{m}$  diameter ( $f/0.88$ ) for operation at  $\lambda = 1 \mu\text{m}$ . The lens functions in free space and has a refractive index of 1.5. Figure 1(a) represents the substrate profile that corresponds to the continuous-phase diffractive lens that satisfies these criteria. The maximum etch depth is 2.0  $\mu\text{m}$ . The response of the lens, determined by the boundary-element technique with TE polarization, is represented in Fig. 2. The diffraction-limited spot size is approximately 2  $\mu\text{m}$ , and the lens diffraction efficiency (the ratio of energy within this window to the total energy that is incident upon the SWDOE) is 77%.

Figure 1(b) is the substrate profile if we assume that the fabrication technology limits the etch depth to 1.0  $\mu\text{m}$ . The center phase that minimizes the quantization error is  $\theta_c = 203.91^\circ$ . Its diffraction efficiency is 63.2%, which indicates a loss of 13.8%. The responses from these two continuous-phase lenses are compared in Fig. 2. The index synthesis function that corresponds to the phase represented in Fig. 1(b) is represented in Fig. 1(c). It is this function that we encode, using binary, subwavelength features.

To determine  $f(x)$  one must invert Eq. (4). We note from Eq. (4) that  $g(x)$  is a low-pass-filtered version of the binary  $f(x)$ . The low-pass spectra of the two functions must therefore match. The problem of determining a binary structure  $f(x)$  whose low-pass structure matches that of the continuous function  $g(x)$  is similar to the design of a (0, 1) binary-amplitude computer-generated hologram.<sup>13</sup> The distinction is, however, that the function  $g(x)$  is related to the desired phase transmission, not to the total complex-wave amplitude

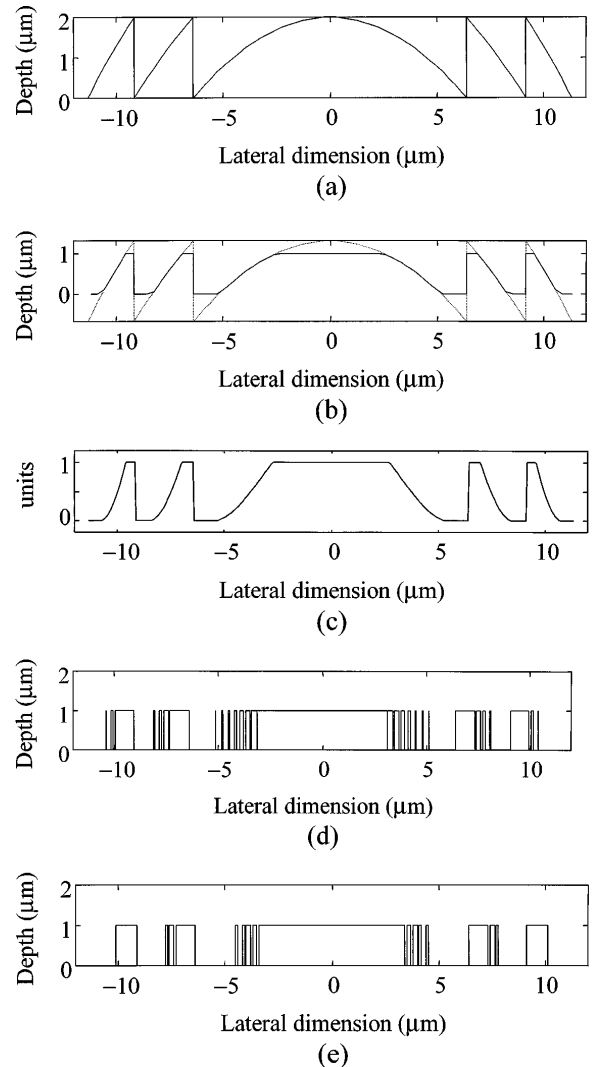


Fig. 1. Binary subwavelength lens design: (a) Substrate profile for  $2\pi$  continuous-phase lens. (b) Substrate profile for  $\pi$  continuous-phase lens. (c) Index synthesis function. (d) Binary subwavelength profile. (e) Spatially quantized subwavelength profile.

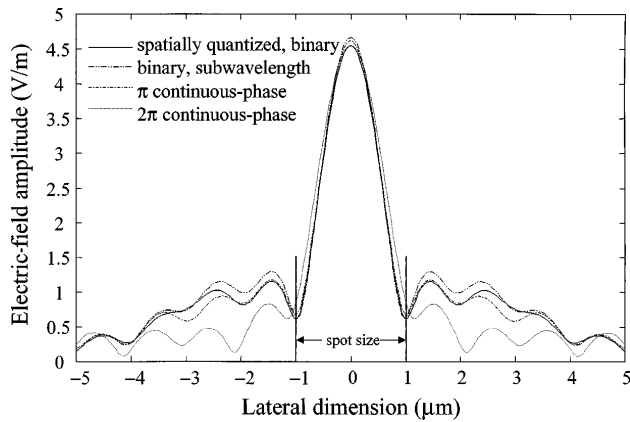


Fig. 2. Electric-field amplitude response for the lenses represented in Fig. 1.

**Table 1. Lens Diffraction Efficiencies for the Subwavelength Design**

Lens Type	Diffraction Efficiency (%)
$2\pi$ -continuous	77.0
$\pi$ -continuous	63.2
Binary subwavelength	59.5
Binary subwavelength, spatially quantized	57.9

transmission. Nonetheless we can rely on the wealth of techniques in the literature, both optimal and suboptimal, to perform the inversion.<sup>13</sup>

As a simple example we use pulse-width modulation to generate  $f(x)$  from  $g(x)$ :

$$f(x) = \sum_{m=0}^{M-1} \text{rect}\left(\frac{x - m\Delta - g_m\Delta/2}{g_m\Delta}\right), \quad (10)$$

where  $g_m = g(m\Delta)$ ,  $m = [0, M - 1]$ , the number of samples  $M = 69$ , and  $\Delta = 0.329 \mu\text{m}$ . The binary structure  $f(x)$  is shown in Fig. 1(d). The diffraction efficiency of this lens is 59.5%, which indicates a loss of only 3.7% owing to subwavelength encoding. The smallest feature  $\delta$  in the structure represented in Fig. 1(d) is 4.8 nm, which ensures that the smallest change in  $g(x)$  can be resolved between adjacent subperiods  $\Delta$ .

However, if we assume that fabrication technology limits the minimum feature  $\delta_{\min}$  to  $0.1 \mu\text{m}$ ,  $f(x)$  must be spatially quantized before it can be fabricated. Spatial quantization of the binary profile in Fig. 1(d) to  $\delta_{\min}$  yields the profile represented in Fig. 1(e). The effect of spatial quantization is to reduce the diffraction efficiency by only 1.6%, to 57.9%.

The diffraction efficiencies for the different lenses are summarized in Table 1. Because our example is meant to be representative and not definitive, we hesitate to draw any general conclusions from the

results. However, it is interesting to note that the most substantial loss in diffraction efficiency arises from the phase quantization that is due to etch-depth limitations.

To recover some of the losses in diffraction efficiency that are due to etch depth and feature size limitations, one can input the lens design in Fig. 1(e) into a vector-based optimization algorithm.<sup>9,14</sup> However, this requires a considerable expenditure of resources, the benefits of which we are still evaluating. We are also evaluating the sensitivity of our procedure to the precompensation of  $\theta(x)$  in Eqs. (7) and (9) and to the encoding of  $g(x)$ . For example, one can use higher-order approximations to the permittivity to refine Eq. (3).<sup>7</sup> We note that the higher-order approximations differ for two-dimensional designs compared with those of one-dimensional designs. However, our zeroth-order approximation is applicable to both.

In this Letter we have presented a detailed procedure for the design of binary diffractive lenses with subwavelength features that to the best of our knowledge is the first of their kind. The procedure uses effective medium theory in combination with a thin phase representation of the diffractive element as its foundation. We have also considered limitations imposed by fabrication, namely, minimum feature size and etch depth, to ensure that the resulting designs can be fabricated.

## References

1. M. W. Farn, *Appl. Opt.* **31**, 4453 (1992).
2. H. Haidner, J. T. Sheridan, J. Schwider, and N. Streibl, *Opt. Commun.* **98**, 5 (1993).
3. D. H. Ranguin, "Subwavelength structured surfaces: theory and application," Ph.D. dissertation (University of Rochester, Rochester, New York, 1993).
4. Z. Zhou and T. J. Drabik, *J. Opt. Soc. Am. A* **12**, 1104 (1995).
5. E. Nojonen, J. Turunen, and F. Wyrowski, *J. Opt. Soc. Am. A* **12**, 1128 (1995).
6. M. Schmitz, R. Bräuer, and O. Bryngdahl, *J. Opt. Soc. Am. A* **12**, 2458 (1995).
7. P. Lalanne and D. Lamerrier-Lalanne, *J. Mod. Opt.* **43**, 2063 (1996).
8. P. Kipfer, M. Collischon, H. Haidner, and J. Schwider, *Opt. Eng.* **35**, 726 (1996).
9. M. Schmitz and O. Bryngdahl, *J. Opt. Soc. Am. A* **14**, 901 (1997).
10. T. K. Gaylord and M. G. Moharam, *Proc. IEEE* **73**, 894 (1985).
11. D. W. Prather, M. S. Miroznic, and J. N. Mait, *J. Opt. Soc. Am. A* **14**, 34 (1997).
12. M. Born and E. Wolf, *Principles of Optics* (Pergamon, New York, 1980), Chap. 14, pp. 705–708.
13. S.-H. Lee, ed., *Selected Papers on Computer-Generated Holograms and Diffractive Optics*, Vol. MS33 of SPIE Milestones Series (SPIE Press, Bellingham, Wash., 1992).
14. D. W. Prather, J. N. Mait, M. S. Miroznic, and J. P. Collins, *J. Opt. Soc. Am. A* **15**, 1599 (1998).